LARGE DISPLACEMENT LINEAR ACTUATOR

Reid A. Brennen, Martin G. Lim, Albert P. Pisano, and Alan T. Chou

Berkeley Sensor & Actuator Center
Electronics Research Laboratory
Department of Electrical Engineering and Computer Science
University of California, Berkeley CA 94720

ABSTRACT

In this paper, a tangential drive (T-drive) polysilicon, linear actuator is presented which produces large magnitude tangential motion by flexing a microstructure in an essentially straight line with moderate input voltage. These devices have been designed, fabricated, and successfully tested to have substantial displacements even for static positioning. The working principle of the T-drive is that the strong electrostatic forces of attraction between a fixed bar and a free bar are converted to large amplitude tangential motion by the parallelogram flexural suspension of the free bar. Operating devices are capable of tangential displacements as great as 32 μm. This displacement is stable and easily varied, since the tangential displacement can be controlled by adjusting the potential between the fixed electrode and the traversing bar. Static displacements are detectable for voltages as low as 15 VDC. Typical T-drives have free bars 200 μm long, 12 μm wide, with flexural suspensions 450 μm long and 2 μm wide. All component thicknesses are 2 μm. Theoretical models for both the flexural suspension and electrostatic forces have been derived and they predict the relation between tangential displacement and excitation voltage.

INTRODUCTION

Within the last two years, several designs of micro-actuators have emerged for specific applications. Among these, one may find shape-memory allow diaphragms for micropumps [1], cantilevered, electrostatically actuated structures to guide probe tips for scanning tunneling microscopes [2], bi-stable mechanical actuators for non-volitile logic elements [3], electrostatic linear actuators for micro friction evaluation [4], a linear micromotor for magnetic disk drives [5], electrostatically-actuated tweezers [6] as well as grippers [7]. A common design theme among these and other micro-actuators are the use of electrostatic, piezoelectric, or shape-memory properties of materials to actuate the micro structures through relatively small displacements (0.01 to 10 μm) with respect to the microactuator size. Although actuation amplitudes and forces for these devices seem to be adequate, the design of higher performance microactuators will require the development of larger amplitude motion with no compromise of actuation force.

Among the electrostatic actuators, one may find two basic designs. The first basic design utilizes parallel plate capacitors with one moving plate that is allowed to displace in the direction of the major field lines, yielding a large-force, small-amplitude actuator. The second basic design utilizes the fringe field of capacitors to drive the moving plate parallel to the fixed plate and perpendicular to the major field lines [8]. This results in a low-force, large amplitude actuator.

In this paper is described the design and performance of a large-force, large-amplitude electrostatic actuator that exhibits the best features of previous electrostatic actuator designs. Thus, the moving capacitor plate is allowed to move parallel to the electric field lines (generating large force) as well as displace parallel to the fixed capacitor plate (generating large amplitude motion). This new electrostatic actuator design utilizes tangential motion of the moving capacitor plate, and thus, is called the T-drive.

Unoptimized designs of T-drive actuators show that low voltage, large force, and large displacement linear actuation is possible.

DESIGN

The force-generating components of the T-drive are made up of two parallel bars which are separated by a small gap. When a voltage is applied across the gap, an electrostatic force is created that acts perpendicular to, and between, the bars. For convenience, this direction is called the normal direction. By fixing one of the bars and attaching the other bar (the free bar) to one side of a parallelogram flexure suspension, Fig. 1, this force can be utilized for motion both parallel and perpendicular to the fixed bar by adjusting the geometry of the suspension. The parallelogram suspension is used in order to constrain the two bars to remain parallel. If the suspension beams of the flexure are not parallel to the normal direction, the total perpendicular force generated, F_{total}, can be decomposed into two force components: one component parallel to and the other component perpendicular to the suspension beams. The tangential force component acts at the end of the flexures and deflects them, resulting in lateral motion of the free bar. This lateral movement can only occur when the initial orientation of the beams is not parallel to F_{total}, i.e. the normal direction. Gravity acting on a simple pendulum serves as an analogy to the concept of the T-drive.

The two critical design features of the T-drive are the flexure geometry, which controls the gap distance as the structure displaces, and the free bar length, which affects the magnitude of the electrostatic force (Fig. 1). The flexure geometry parameters include the offset angle of the beams, the beam dimensions (length, width, and thickness), and the initial gap distance between the free and fixed bars. Larger initial angles of the beams result in a more rapid decrease in gap width and a more rapid increase in applied force as the free bar moves laterally. However, if the initial angle is too large, the free bar will contact the fixed bar as it displaces, and thus short the circuit preventing further movement. The rate of approach of the free bar toward the fixed bar is a function of beam length. The initial gap between the bars determines whether the bars will contact and, if so, what maximum actuator displacement is possible before they meet. The width, thickness, and length of the beams determine the stiffness of the flexure suspension and the magnitude of F_{total} is proportional to the free bar length.

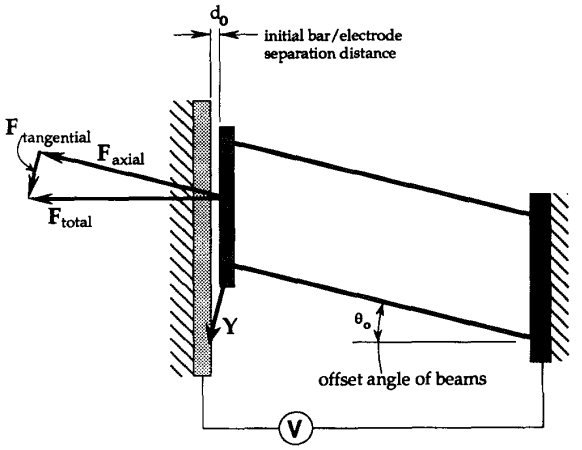

Figure 1

Schematic of Tangential Drive Linear Actuator. Note that it is $F_{tangential}$ that deflects the structure in the Y-direction.

CH2783-9/90/0000-0135$01.00©1990 IEEE

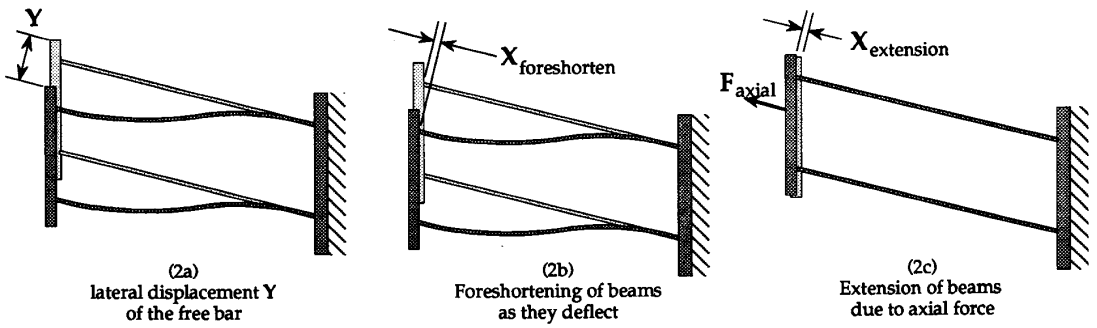

(2a) lateral displacement Y of the free bar

(2b) Foreshortening of beams as they deflect

(2c) Extension of beams due to axial force

Figure 2
Types of beam displacements
(Shaded structures are in displaced position)

THEORY

Using a modified parallel-plate capacitance model, the total electrostatic force F_{total}, generated between the facing sides of the bars is estimated by:

$$F_{total} = C_1 \frac{\varepsilon_o A}{2}\left(\frac{V}{d}\right)^2 \qquad (1)$$

where A is the capacitor plate area, V is the applied potential, d is the gap between the bars, ε_o is the permittivity of air, and C_1 is a constant factor. The factor C_1 is based on results from a electrostatic finite element package, Maxwell [9] and improves the estimate for F_{total} by including fringe fields in the capacitance analysis. For our model, C_1 is set to 1.15. Clearly the factor, C_1 must be recalculated if the design of the device is modified.

As the free bar moves laterally, it approaches the fixed bar. The rate of approach is governed by three separate phenomena (Fig. 2). The first, due to the initial angle of the support beams, is the approach of the free bar as it moves laterally a distance Y (Fig. 2a). The second is the foreshortening, X_f, in the *axial* direction, of the support beams as they deflect (Fig. 2b). The third is the axial extension, X_e, of the support beams as the axial component of the total force is applied (Fig. 2c). If θ_o is the angle of the beams with respect to the normal direction, then the gap, d, can be expressed as:

$$d = d_o - Y\sin\theta_o + (X_f - X_e)\cos\theta_o \qquad (2)$$

where d_o is the initial gap. Using small displacement beam theory, expressions for Y, X_f, and X_e can be derived [10], and, expanding each of the terms in Eq. 2:

$$d = d_o - \frac{F_{total} L \cos^2\theta_o}{b\ t\ E} \qquad (3)$$

$$+\frac{\tan\theta_o \sin\theta_o}{4\lambda}\left\{-\lambda L\left(1+\gamma^2\right)+\sinh(\lambda L)\left[\cosh(\lambda L)\left(1+\gamma^2\right)-2\gamma\sinh(\lambda L)\right]\right\}$$

$$\text{where } \gamma = \frac{\cosh(\lambda L) - 1}{\sinh(\lambda L)} \qquad (4)$$

$$\lambda = \left[\frac{F_{total}\cos\theta_o}{EI}\right]^{\frac{1}{2}} \qquad (5)$$

and L is the length of the flexure beams, b is the width of the beams, t is the thickness of the beams, E is Young's modulus of elasticity for polysilicon, and I is the area moment of inertia of the beams.

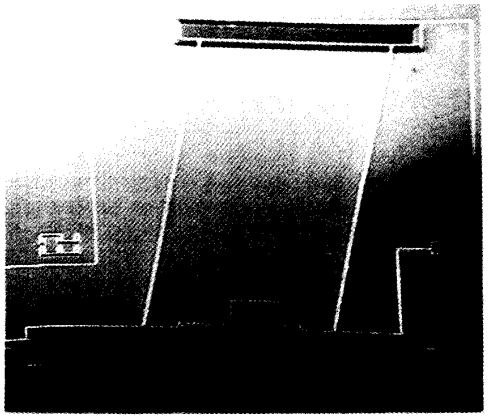

Figure 3
SEM of a single bar T-drive structure. The L-shaped breakaway support is removed before testing.

Figure 4
SEM of the free bar of a single bar T-drive. The scale and pointer can be seen between the two suspension beams on the left. The dimples can be seen in the center of the free bar. Note the vertical side walls of the polysilicon in the gap.

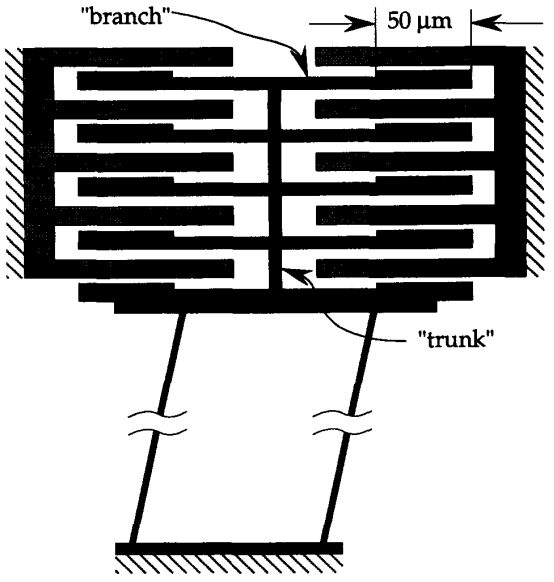

Figure 5
Schematic of Multiple bar T-drive Structure
Note the 50 mm long sections on each branch which act as the parallel plate attractors.

By solving equations (1) and (3) simultaneously, values for F_{total} and d can be found for given values of the applied voltage V. Once F_{total} is known, the lateral displacement Y of the free bar can be determined, by:

$$Y(F_{total}) = \frac{\tan\theta_o}{\lambda}\left[\lambda L - \sinh(\lambda L) + \frac{(\cosh(\lambda L) - 1)^2}{\sinh(\lambda L)}\right] \quad (6)$$

Two designs were implemented to demonstrate the T-drive concept. The first design was very similar to the schematic in Fig. 1. This design used a single free bar attached to the parallelogram suspension (Figs. 3 and 4). In this design, the electrostatic attracting force is linearly proportional to the length of the free bar. The second design increased the effective bar length by using multiple free bar/fixed bar pairs which form a "tree" (Figs. 5 and 6). The odd-shaped bars or "branches" attached to the central "trunk" of the tree of the suspension each have a wider 50 μm long section which has a 2 μm distance from the free bar. All other parts of the branch, including the back side of the 50 μm section were separated by a distance of at least 6 μm gap from the fixed bars. In this manner, the 50 μm section acted as a constant attraction surface area; as the structure displaced, the effective area of the parallel "plates" did not change.

Both of the structure types used a scale and pointer method to measure displacements. Due to the long overhang lengths of the structures, sometimes as great as 600 μm long, breakaway supports were used to provide added stiffness to the structure during fabrication (seem in Fig. 3). The breakaway supports were mechanically removed by physically rupturing them with test station probes. Small dimples were introduced into the free bars to prevent large area contact between the free bars and the substrate, thereby keeping the released structure free from surface tension adhesion during rinsing and drying.

FABRICATION and EXPERIMENTAL METHODS

The structures were fabricated using the process developed by Lim [4]. The structural layer defining the device was 2 μm thick phosphorus-doped polycrystalline silicon. The T-drive structures were fabricated with 1.7 μm wide, 400 and 446 μm length beams and with beam angles ranging from 4.6° to 5.2°. The initial gap between the free and fixed bars was 2.1 μm. A ground plane was used beneath the free bar and its suspension to prevent electrostatic interference from the substrate.

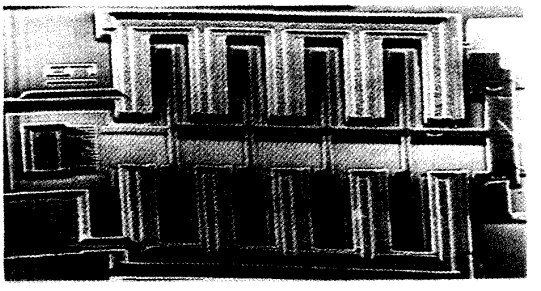

Figure 6
SEM of the free bar component of a multiple bar T-drive.

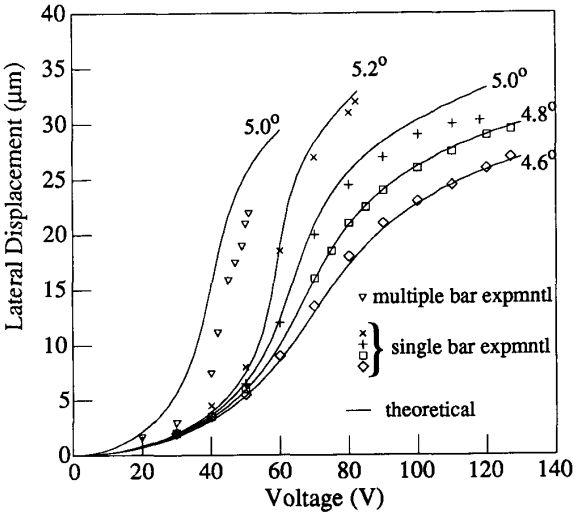

Figure 7
Lateral displacement Y versus applied voltage for various T-drive structures. The corresponding angle of the beams with respect to the primary direction is shown next to each set of data.

Static displacement measurements as a function of applied voltage were performed for several structures by use of the scale and pointer. This method allowed a ± 0.5 μm accuracy. The applied voltages ranged from 0 to 127 V. Out-of-plane deflections of the free bar were made using a microscope focusing method with an accuracy of about ±2 μm for small deflections. All testing was performed in air observed under under 1000X magnification both directly through a microscope and on a video monitor. The beam widths of the structures were measured using SEM images.

RESULTS and DISCUSSION

The theoretical determination of static displacement was dependent on the accuracy of both Young's modulus and the suspension beam widths. After measuring the beam widths, the value of Young's modulus used in the theoretical model was varied until theoretical displacements were found that corresponded to the experimental data. Using this method, the Young's modulus was found to be 105 ±15 GPa.

Static displacement amplitudes as a function of voltage were measured for several single and multiple bar structures and are plotted in Fig. 7. The displacements of the structures were smoothly controlled by varying the voltage. The T-drive designs with larger suspension beam angles deflected more for a given voltage. The larger beam angle resulted in a larger tangential component of the total electrostatic force

Table 1 Maximum Displacements attained for Single and Multiple-Bar T-drive structures each with its beams at different angles with respect to the normal direction.

Maximum displacement (μm) (voltage at maximum displacement)				
	Angle of beams			
	4.6°	4.8°	5.0°	5.2°
single bar T-drive (446 μm beam)	27.0 (127V)	29.5 (127V)	30.5 (118)*	32.0 (82V)*
Multiple bar T-drive (446 μm beam)	22.0 (57V)†	20.0 (53V)†	22.0 (50)†	21.0 (45)†

* At higher voltages, the free bar contacted the fixed bar.

† At higher voltages, one of the branches deflected and contacted the fixed bar.

since $F_{tangential} = F_{total} \sin\theta$. This larger $F_{tangential}$ reduced the gap more for a given voltage than that of the lesser-angle beam designs. This increased F_{total} and correspondingly, $F_{tangential}$. Consequently, the displacements of the larger angle beam designs increased faster than the lower voltage designs as the voltage was increased.

For a given voltage, the single bar structures deflected less than the multiple bar structures. The experimental results bear out the expected proportionality between the length of the attracting surfaces (i.e. the bar lengths) and F_{total}.

The maximum static displacement amplitudes attained for the structures are shown in Table 1. For an applied voltage of 127V, a static displacement of 32 μm was measured for a single bar T-drive with 446 μm beams at an angle of 5.2°. The 32 μm displacement was the greatest displacement measured for any of the T-drive structures. The maximum displacement increased with an increase in θ_0. Geometrical constraints limited the maximum displacement of the structures with large θ_0. In these cases the bars contacted before the voltage reached 127V.

There was a significant difference between the maximum attainable displacements of the single and multiple bar structures. The multiple bar design of the tree end was inherently more compliant than the single bar structures. It was noted during testing that the branches deflected towards their respective fixed bars due to the large forces generated as the gap became smaller. When the gap decreased to a certain amount, the force balance between the electrostatic force and the resisting force in one of the branches would become unstable and the branch contact the fixed bar. The complexity of the "tree" may have contributed to the less than predicted displacements.

During testing of the single and multiple bar T-drives, it was noted that the free bar section of the devices levitated out of plane. The amplitude of the levitation varied from device to device depending on the physical dimensions of each device. For most of the devices, the out-of-plane levitation increased as the applied voltage increased until about 30 V was reached, after which the levitation decreased and was not perceptible above about 50 V. This levitation is due to the interaction of the ground plane and the free and fixed bars [11].

Theoretical calculations reveal that the forces that the T-drive would be able to generate are dependent on how much the suspension has been displaced before the force is exerted. This effect is due to the elastic forces required to deflect the suspension. For example, for one multiple bar design, an initial displacement of 10 μm would require approximately 36V (Fig. 8). Assuming the structure at this point contacts the the structure upon which it acts and the T-drive does not displace further, an increase of 8V would provide a force of 2 μN (1 μN is the force exerted by a 350 μm cube of silicon in gravity). Lower initial displacements reduce the rate at which the applied force would increase with voltage.

The differences in displacements between the theoretical model and the experimental data can be attributed to several causes. First, the structures not only have compliant suspension beams, but the free bars could also deform. As noted above, this was of especial concern for the multiple bar T-drive. Further, in the multiple bar free bar/fixed bar design, only part of each branch was near to the fixed bar, the nominal gap being 2 μm. However, the branch was surrounded by other features that were about 6 μm distant that were at the opposite potential. Since an electrostatic force was generated by this gap, the total force was actually less than the theoretical force.

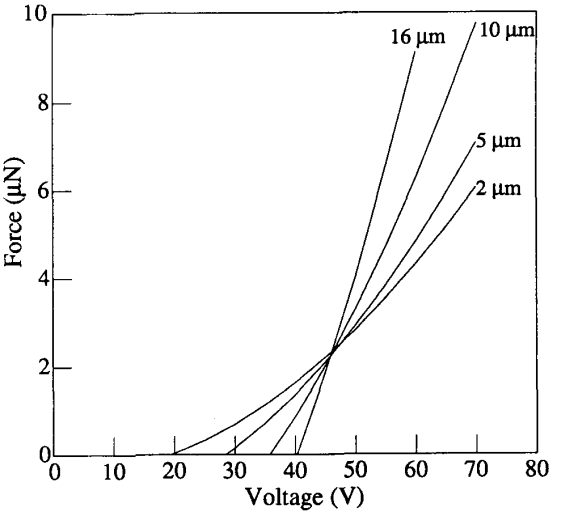

Figure 8
Theoretical force exerted by the T-drive versus applied voltage at fixed lateral displacements. The fixed displacement is noted by each curve.

The model had several limitations. As noted above, the beam theory used to describe the T-drive suspension was valid only for small displacements, or more accurately, for small changes of slope of the beams. These T-drive suspension beams did have significant changes of slope when they deflected. The effect of this increased slope was to effectively increase the stiffness of the system [12]. A second limitation of the model was that the model assumed perfect geometric dimensions whereas the actual structures had dimensions that varied slightly with the fabrication process. Since large displacements only occurred when the gap had become very small, the uniformity of the gap was very important.

The motion generated by the T-drive is not perfectly linear, but since the free bar travels in a very large radius arc as the beams deflect, but this non-linearity is very small.

CONCLUSION

Electrostatic large displacement structures have been developed, fabricated, and tested. The T-drive concept demonstrates that direct electrostatic attraction can be used to generate large displacements. These structures attained static displacements of up to 32 μm with an applied voltage of 82V and 22 μm with an applied voltage of 50V. Structures with longer beams show promise for even greater displacements. A theoretical model has been developed which closely describes the experimental data. Using this model, a value has been calculated for Young's modulus of 105 GPa. Further, it has been shown that relatively large forces can be applied with small increases in voltage once the free bar undergoes a large displacement and the gap between the free and fixed bars is reduced.

ACKNOWLEDGEMENT

The authors would like to thank the industrial members of the Berkeley Sensor & Actuator Center for the support and funding provided for this project.

REFERENCES

[1] J.D. Busch and A.D. Anderson, "Prototype Micro-Valve Actuator", *Proc. IEEE Micro Electro Mechanical Systems Workshop*, Napa Valley, CA, Feb. 1989.

[2] S. Akamine, T.R. Albrecht, M.J. Zdeblick, and C.F. Quate, "Microfabrication of Integrated Scanning Tunneling Microscopes", *Transducers '89, 5th International Conference on Solid-State Sensors and Actuators*, Montreux, Switzerland, 25-30 June 1989.

[3] P.L. Bergstrom, T. Tamagawa, and D.L. Polla, "Design and Fabrication of Micromechanical Logic Elements",*Proc. IEEE Micro Electro Mechanical Systems Workshop*, pp. 15-20, Napa Valley, CA, Feb. 1989.

[4] M. G. Lim, J. C. Chang, D. P. Schultz, R. T. Howe, and R. M. White, "Polysilicon Microstructures for Characterize Static Friction." *Proc. IEEE Micro Electro Mechanical Systems Workshop*, pp. 82-88, Napa Valley, CA, Feb. 1989.

[5] Martin G. Lim, Roger T. Howe, and Roberto Horowitz, "Design and Fabrication of a Linear Micromotor for Magnetic Disk File Systems", ASME Winter Annual Meeting, San Francisco, December 10-15, 1989

[6] L. Y. Chen, Z. L. Zhang, J. J. Yao, D. C. Thomas, and N. C. MacDonald, "Selective Chemical Vapor Deposition of Tungsten for Microdynamic Structures," *Proc. IEEE Micro Electro Mechanical Systems Workshop*, pp. 82-87, Salt Lake City, UT, Feb. 1989.

[7] Chang-Jin Kim, Albert P. Pisano, Richard S. Muller, and Martin G. Lim, "Polysilicon Microgripper", *to be presented at IEEE Solid-State Sensor and Actuator Workshop*, Hilton Head Island, South Carolina, June 4-7, 1990.

[8] William C. Tang, Tu-Cuong H. Nguyen, Michael W. Judy, and Roger T. Howe, "Electrostatic-Comb Drive of Lateral Polysilicon Resonators", *Transducers '89, 5th International Conference on Solid-State Sensors and Actuators*, Montreux, Switzerland, 25-30 June 1989.

[9] Ansoft Corporation, Pittsburgh, PA 15123 *Maxwell Users Guide*, January, 1989

[10] Raymond J. Roark and Warren C. Young, Formulas for Stress and Strain, 5th Ed., McGraw-Hill, New York, 1975

[11] William C Tang, Martin G. Lim, and Roger T. Howe, "Electrostatically Balanced Comb Drive",*to be presented at IEEE Solid-State Sensor and Actuator Workshop*, Hilton Head Island, South Carolina, June 4-7, 1990

[12] Egor P. Popov, Introduction to Mechanics of Solids, Prentice-Hall, Inc., Englewood Cliff, New Jersey, 1968